MATERIALS PHYSICS AND MECHANICS RESEARCH ARTICLE

Submitted: April 22, 2025 **Revised:** May 13, 2025 **Accepted:** July 10, 2025

Polymer weld characterization and defect detection through advanced image processing techniques

G.C. Ganesha [1,2], **C. Mukti** [1], **S. Arungalai Vendan** [1]✉, **R. Sharanabasavaraj** [1]

[1] Dayananda Sagar University, Bangalore, India

[2] Dayananda Sagar College of Engineering, Bangalore, India

✉ arungalaisv@yahoo.co.in

ABSTRACT

Welding defect detection in a radiographic image is vital in industrial non-destructive testing. It is significant in evaluating weld anomalies and surface and subsurface imperfections in welded joints. Digital image processing techniques can make automation feasible in the weld microscopic image interpretation, thus reducing the instances of observational human errors in weld inspection. This technique will give more reliability, speed and reproducibility to the inspection system. This paper uses MATLAB image processing tools for weld defect detection using scanning electron microscope images of ultrasonically welded polymer samples. Image processing features of gray scaling, image resizing, histogram equalization, edge detection, thresholding, filtering, texture analysis, and image segmentation have been implemented for the detection and characterization of defects in weld scanning electron microscope images. Thorough insights into the structure of these defects are an essential step in appreciating the weld's quality. The approach is well-suited for defect detection of any welding technique.

KEYWORDS

image processing • weld defects • scanning electron microscope analysis

Acknowledgements. *The authors thank Mr. Alwin Raj Lobo, Head, UltraTechSonic Solutions, Bangalore, for extending research facilities to undertake this project.*

Citation: Ganesha GC, Mukti C, Arungalai Vendan S, Sharanabasavaraj R. Polymer weld characterization and defect detection through advanced image processing techniques. *Materials Physics and Mechanics*. 2025;53(3): 48–68.

http://dx.doi.org/10.18149/MPM.5332025_5

Introduction

Basic structure and mechanical or physical properties of weld gets affected due to the varying imperfections and irregularities that may appear in a weld. The weld defects can be categorized into superficial and internal defects, depending on the location of the defect. Control of welding quality and reliability is significant for industrial activities like component manufacturing and structure assembly. Significant functional abnormalities may result as a consequence of the welding anomalies. Defect detection is considered particularly challenging owing to the factors like insufficient contrast, the noised nature of the radiographic film, or the reduced geometric dimensionality of irregularities. Radiography provides detailed internal visualization of the welds and enables manufacturers to verify compliance with safety standards, specifications, and manufacturing codes.

Image processing refers to the manipulation and analysis of digital images using a variety of algorithms and methods. Digital image processing techniques are employed to automate defect detection and identification, enhance visual representation of data, and standardize radiographic analysis methods, thereby increasing their reliability and consistency. Digital image processing covers improving and extracting intrinsic details from digital images and results in the generation of new images or specific assessments from the images. To consider the elaborations in micro-imaging and for accurate indication of the discrepancy, appropriate preprocessing and segmentation methods need to be selected. Reproducibility and reliability of results are the essential requirements in the automation of non-destructive testing, mainly in image characterization, to be at par with human judgment. This work aims to identify anomalies and defects like porosity, cracks, lack of penetration, etc., using image processing of welded joint microscopic images.

The proposed MATLAB-based image processing system is well-suited for real-time deployment in manufacturing environments. It can interface with industrial cameras and data acquisition systems using the Image Acquisition Toolbox for continuous monitoring. MATLAB code can be compiled into standalone applications or converted to C/C++ for integration with embedded systems and industrial control platforms like PLCs and SCADA. The system supports edge computing through lightweight, optimized pipelines deployable on devices like Raspberry Pi or NVIDIA Jetson. Real-time performance is achieved using techniques such as ROI detection, frame skipping, and GPU acceleration. Additionally, the system can be integrated into production lines to automate actions such as triggering alarms, rejecting defective parts, and logging inspection data.

MATLAB trains a supervised learning model using extracted features and labels, common classifiers are as follows: fitcsvm – support vector machine (good for small datasets); fitcknn – k-nearest neighbors; fitctree – decision tree; trainNetwork – for CNN-based classification (deep learning toolbox).

State of the art in image processing for welding defect detection

Intensive research contributions are made to resolve the discrepancies in the image processing techniques utilized for weld image characterization. Xu Y. et al. [1] proposed an enhanced Canny edge detection algorithm based on their analysis of the gray gradient in the weld image. Results showed that real-time seam tracking objectives can be met by precisely controlled image processing. Nacereddine N. et al. [2] proposed a few variations in the image processing sequence significant for effective defect detection in images. The process is initiated by concentrating on the region of interest (ROI) to ensure a targeted analysis. A median filter is applied to minimize noise and enhance image quality, vital for accurate assessments. Dynamic stretching and local contrast enhancement improve clarity across various backgrounds, facilitating effective feature extraction. Finally, the Otsu method is utilized to optimize segmentation, allowing for precise identification of defects. In 2009, Liao G. and Xi J. [3] proposed a pipeline welding machine image detection method using the largest variance threshold method to establish adaptive segmentation. The process converts images to black and white, removes small noise, and utilizes level projection for efficient real-time defect detection and quality inspections. In 2007, Yang S.M. et al. [4] employed automation in Metal Inert Gas welding using a CCD camera with a laser stripe for seam tracking and adaptive Hough transformation for weld point extraction. A generalized delta rule algorithm-based neural network optimizes welding parameters, with joint width and depth as inputs from the images and is observed to influence overall weld quality significantly. Roca Barceló F. et al. [5] introduced an automated system using TOFD, image processing, and neural networks for accurate weld defect detection and classification. The TOFD method has a drawback associated with the appearance of speckle noise.

In 2020, Li Y., Hu M. and Wang T. [6] presented a deep learning-based weld seam image recognition algorithm using the Adam adaptive moment estimation for efficient convolutional neural network training. The adaptive threshold method for weld seam extraction was tested on 4500 tube images, and the results show effective identification and classification of weld defects in terms of parameters like false detection rate, recall rate, and overall accuracy. Pan H. et al. [7] developed a novel approach using MobileNet feature extractor and leveraged a pre-trained deep learning architecture, originally optimized for diverse image recognition tasks, to extract key features for identifying welding defects. By integrating an additional classification layer, this hybrid model significantly outperformed other comparable methods, achieving an impressive accuracy rate of nearly 98 %. In 2019, Sun J. et al. [8] presented a machine vision algorithm for detecting and classifying weld defects in thin-walled canisters. Using a modified background subtraction method, the algorithm achieves over 99 % accuracy in real-world applications, proving effective for real-time and continuous weld defect detection. In 2002, Wang G. and Liao T.W. [9] developed an automatic computer-aided system for identifying welding defects using background subtraction and histogram thresholding techniques. In 2016, Ranjan R. et al. [10] used specific defect features like vertical intensity plot and defect spread region for weld defect identification, with respect to its location and severity, and classification into different kinds of imperfections or irregularities. In 2020, Kumar R.K. and Omkumar M. [11] explored the ultrasonic plastic welding of high-performance polyamides (HPPA) matrix composite. It is a glass-filled semi-crystalline and partially aromatic polyamide composite for automotive applications. A weld strength of 3.1 kN was achieved, with minimal voids and negligible weight loss. Key findings include decreased glass transition temperature and suitable degradation temperature for high-temperature applications. In 2019, Mohammad E.J. et al. [12] utilized the K-means method for optimal thresholding, showing sensitivity to small datasets but improved performance with larger datasets, especially when the number of clusters is minimal.

In 2023, Shaikh K. et al. [13] presented a hybrid architecture that uses a multilayer perceptron (MLP) for feature extraction and combines it with classical classifiers like random forest (RF) and support vector machines (SVM). Applied to wheel conicity defect detection, the MLP-RF combination yielded the best performance with up to 99 % accuracy. The hybridization allows for efficient learning from both structured sensor data and statistical features, making it suitable for mechanical fault diagnosis. In 2024, Tata R.K. et al. [14] proposed a hybrid convolutional neural network (CNN) and long short-term memory (LSTM) model. CNN extracts spatial features from surface images, while the LSTM captures temporal relationships (e.g., variations across sequences or production cycles). The hybrid model improves defect detection accuracy by ~ 20 % and reduces false positive rates by ~ 30 %, making it suitable for time-series-based industrial inspection tasks such as continuous casting or rolling. In 2024, Wang X. et al. [15] addressed the challenge of detecting defects on dense IC surfaces, where information imbalance and micro-defects make detection difficult. A hybrid model combining ResNet50 and Vision Transformer (ViT) is developed. ResNet handles low-level feature extraction, while ViT captures long-range dependencies. The model achieves 98.6 % accuracy, outperforming standalone CNN or ViT architectures, and is particularly effective for microelectronic manufacturing.

The accuracy of defect detection using MATLAB-based image processing depends on several factors, including the type of defect, image quality, features used, classifier, and preprocessing methods. However, based on published studies and typical results from academic and industrial projects, Table 1 lists a few of the reference points [13–15].

Table 1. Accuracy in % for various techniques used for image defects detection

Application area	Defect type	Technique	Accuracy (approx.), %
Weld inspection	Cracks, voids, inclusions	LBP + SVM / Edge detection + Morphology	85–95
Composite materials	Delamination, air voids	GLCM + CNN / Ultrasound image processing	90–97
Metallic surfaces	Scratches, dents, porosity	Texture + Intensity histograms + Decision tree	80–90
PCB / Solder joints	Missing pads, solder bridges	Template matching + Thresholding	88–93

Table 2. Comparison of MATLAB based image processing with baseline methods

Aspect	Baseline methods (e.g., manual inspection / traditional thresholding)	Proposed MATLAB-based approach
Automation	Manual or semi-automatic, subjective, time-consuming	Fully automated using algorithms such as edge detection, morphological operations, or machine learning
Accuracy	Typically lower due to human error and inconsistent criteria	Higher accuracy by using optimized filters and algorithm tuning
Noise handling	Poor tolerance to lighting, contrast, or texture noise	Robust pre-processing steps (Gaussian filtering, histogram equalization, etc.) remove noise effectively
Feature extraction	Manual or limited to basic statistics	Advanced techniques: texture analysis (e.g., LBP, GLCM), shape descriptors, color segmentation
Defect classification	Usually not implemented or rule-based	Incorporates ML models (SVM, KNN, decision trees) trained on defect features
Consistency & repeatability	Varies with operator and condition	Highly consistent, script-based processing ensures reproducibility
Processing time	Slower and subjective	Faster with batch processing using MATLAB scripts/functions

In MATLAB-specific workflows, using local binary pattern (LBP) or GLCM (gray-level co-occurrence matrix) for feature extraction and SVM or KNN for classification, the accuracy typically ranges from 85 to 95 %. When combined with image augmentation and proper labeling (using Image Labeler), detection rates can improve by 5–10 %. MATLAB's deep learning toolbox (e.g., using pre-trained CNNs like AlexNet or ResNet with transfer learning), gives 95 %+ accuracy when sufficient labeled data is available. Performance comparison of MATLAB-based Image processing with other baseline methods is described in Table 2.

The proposed MATLAB-based image processing approach demonstrates superior performance compared to traditional thresholding and edge-based methods, as evident in higher classification accuracy (91.4 vs. 72.3 %), and improved robustness to noise and lighting variations. The integration of texture-based feature extraction (e.g., LBP) and machine learning classifiers significantly enhances the defect detection capability across multiple defect types.

Experimental work and image processing analysis

Preprocessing stage

The basic initiation in image processing is the initial set of operations performed on raw image data to prepare it for further analysis or processing. The goal of preprocessing is to enhance the quality of the image and to remove any distortions or irrelevant information that may hinder subsequent tasks.

This stage involves the following operations to be performed to prepare the image for further extraction of defect information:

1. Histogram equalization is a technique for improving an image's contrast by adjusting the histogram's intensity distribution. This method enhances the image's visibility and detail by spreading the most frequent intensity values. Histogram equalization is a powerful and widely used technique for enhancing image contrast, making it a fundamental tool in various image processing applications. The image's histogram is computed, a plot of the number of pixels for each intensity level (from 0 to 255 for an 8-bit image).
2. Resizing of Images: By resizing images appropriately, you can balance maintaining sufficient detail for analysis while optimizing computational and storage resources. This balance enhances the efficiency, effectiveness, and applicability of image-processing techniques across various domains.
3. Gray scaling transforms a color image into shades of gray. This involves reducing the image's depth from full color (usually 24-bit RGB) to 8-bit grayscale. In a grayscale image, each pixel represents a shade of gray, varying from black (0 intensity) to white (255 intensity). For each pixel, the intensity of the gray shade is calculated using the formula: Gray=$0.299\times R+0.587\times G+0.114\times B$ [2].

The following are the Inferences that can be drawn from the grey scaling mechanism:

1. Consistent gray levels across the weld bead indicate a consistent welding process.
2. Inconsistent gray levels may suggest issues such as varying penetration, inconsistent heat input, or changes in welding speed.
3. Dark spots can indicate porosity or voids within the weld. Darker areas usually represent areas of lower density.
4. Light spots or Brighter areas may indicate inclusions or areas of higher density. They could also point to overheating or burning through the material.
5. The gradient of gray Levels indicates the HAZ, which has a gradual transition from the base metal to the weld metal. Sharp changes in gray levels can indicate improper heat control.

6. Proper penetration is indicated by a consistent gray level throughout the weld depth.
7. Insufficient Penetration appears as a lighter gray area in the center of the weld cross-section, indicating the weld did not fully penetrate.
8. Cracks appear as distinct lines or streaks within the grayscale image, often darker than the surrounding material.

The study reviewed methods like image enhancement, segmentation, and machine learning techniques. The research highlighted the effectiveness of these approaches in identifying defects and imperfections. The research observation underscores the role of image processing in improving weld inspection quality. The work carried out in this research reflects on the advancement in the image processing technique for weld defect detection of polymer samples joined using ultrasonic welding. The stages of the image processing technique are illustrated in the flowchart, Fig. 1.

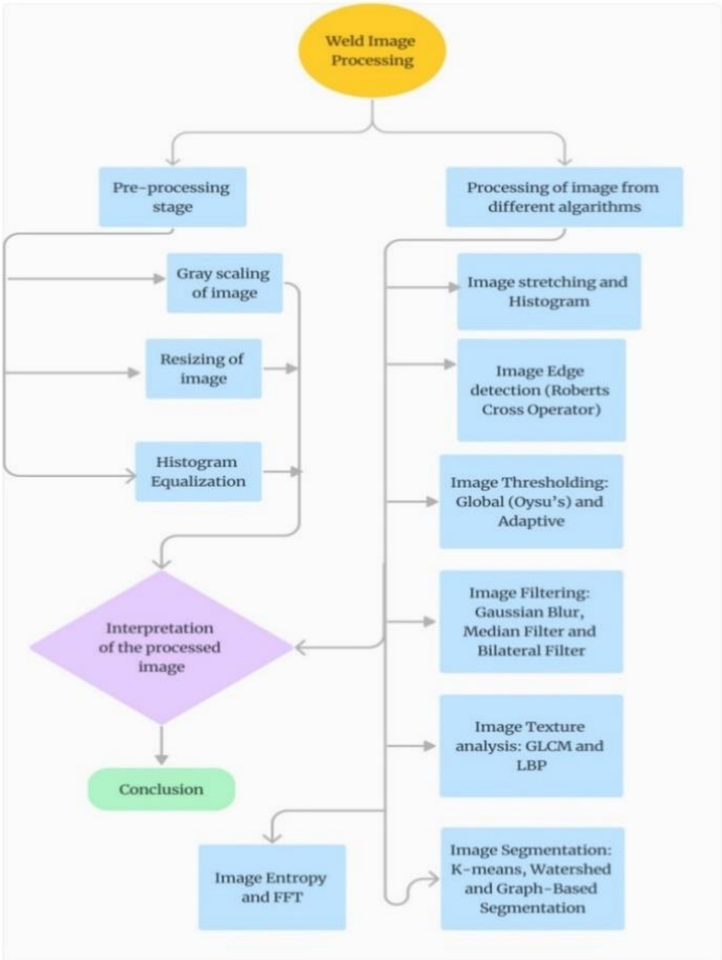

Fig. 1. Flowchart showing the stages of image processing adopted

Image processing was carried out with the scanning electron microscopy (SEM) images of the polymer weld samples. The polymer material is ABS, and the two parts of ABS are joined using ultrasonic welding. The ultrasonic welding involves providing ac supply at 240 V and 50 kHz to the piezoelectric crystal. This results in the generation of high-frequency mechanical vibrations, which are then transmitted to the weld material through the sonotrode and a horn, Fig. 2.

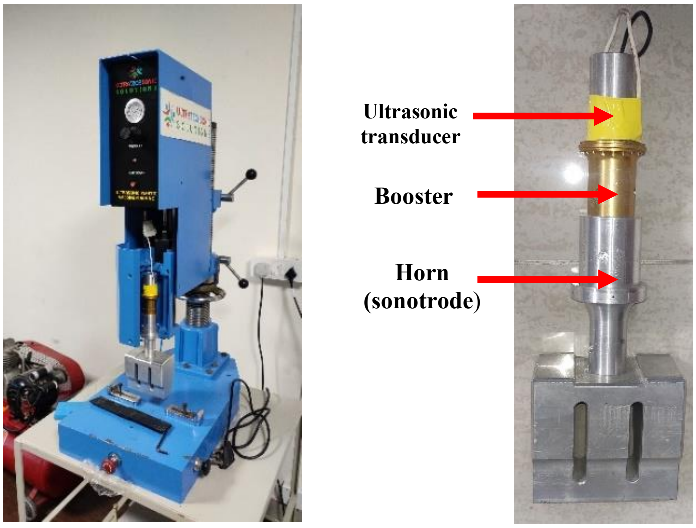

Fig. 2. Images of Ultrasonic weld machine, transducer, sonotrode (booster), horn assembly

The sonotrode horn also transmits and exerts static pressure on the weldment, apart from the vibrations generated in the piezoelectric converter. The horn is customized to suit the weld geometry, and the welding machine has parameter settings for the weld requirements. The parameters of importance are weld time, hold time, amperage corresponding to the energy requirement, and static pressure. The experimental work involved trials with different settings of the process parameters based on trial and error, and also based on the expertise of the technicians at UltraTech Sonic Solutions, Basavangudi.

Table 3. Operating values of parameters and weld status for ABS Material (N.W - no weld, P.W - partial weld, G.W - good weld with high strength, DT - destructive testing)

Sl. No	Test identification	DT, s	Weld time, s	Holding time, s	Current, mA	Pressure, Bar	Power, Watts	Weld status based on DT*
1	1A	0.55	0.15	0	0.1	2	1	N.W
2	1B					2	1	N.W
3	1C					2	1	N.W
4	2A	0.55	0.3	0	0.2	2	1	N.W
5	2B					2	1	N.W
6	2C					2	1	N.W
7	2D	0.55	0.3	0	0.2	3	2	N.W
8	2E							N.W
9	2F							N. W
10	3A	0.55	0.4	0	0.3	4	3	P.W
11	3B							P.W
12	3C							P.W
13	3D	0.55	0.5	0	0.3	4	3	G.W
14	3E							G.W
15	3F							G.W
16	3G	0.55	1	0	0.6	5	4	G.W.H
17	3H			0	0.6	5	4	G.W.H
18	3I			1	0.8	5	5	Overburn

The process parameter variation considered for this work has been listed in Table 3. The weld status has been provided based on the destructive testing on the weld samples.

Scanning electron microscopy (SEM) imaging of various samples provides insights into the effects of thermal gradients caused on the weld surface due to generated friction and viscous heating of the acrylonitrile butadiene styrene (ABS) material at various points of the joint formation. As the first step, a microscopic image of the base ABS material, without welding, was captured, serving as the basis of comparison with the SEM of the welded material sample.

Image processing was carried out in MATLAB ver.23a. The flowcharting (Fig. 3) highlights the methodology used in segmentation and feature extraction algorithms adopted to extract the morphological and image intensity features of the SEM images.

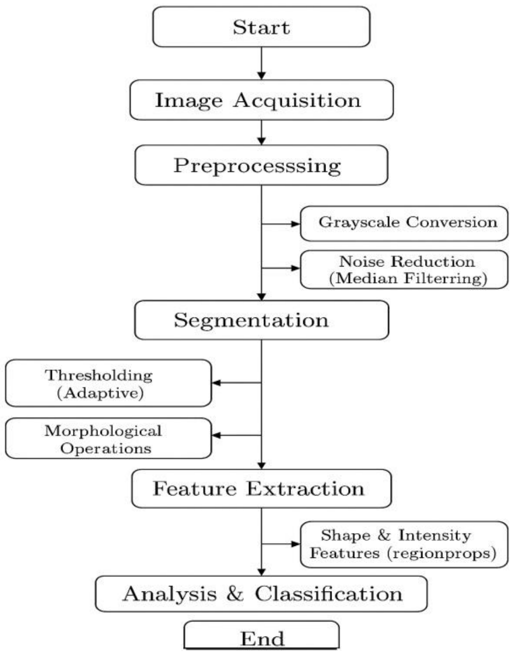

Fig. 3. Methodology of the segmentation and feature extraction

Similar processes have been adopted for algorithms such as texture analysis, entropy, FFT, and filters to extract the various properties of the images. For labeling, MATLAB’s image labeler toolbox is used to manually annotate cracks and voids on the input images. Each defect was marked using bounding boxes or pixel-level masks, depending on its complexity and size. The annotated data was saved in ROI and label data formats compatible with supervised machine learning workflows in MATLAB. This labeled dataset served as the basis for training and evaluating defect classification models. The following analyses were performed on the SEM images of the polymer weld samples [16–23].

1. The histogram is utilized to reveal quality issues for the welded images. The overall position of the histogram along the x-axis indicates the image's brightness. If the histogram is skewed towards the left, the image is predominantly dark. If it is skewed towards the right, the image is predominantly bright. The contrasting features of the image are captured by the histogram span. A wide histogram that covers a broad range

of intensity values suggests high contrast, while a narrow histogram suggests low contrast. Uniform and expected distributions may indicate good-quality welds, while unexpected spikes or gaps could indicate defects or inconsistencies.

2. Edge detection: it enables the identification and location of critical discontinuities in the weld by variations in intensity or color introduced into the image. These discontinuities often represent the boundaries of objects within the image.

Weld seam identification. Continuous seam: A well-defined, continuous edge indicates a consistent and smooth weld seam, which indicates good quality. Gaps or discontinuities: breaks or gaps in the edge detection output may indicate defects such as cracks, incomplete fusion, or lack of penetration.

Weld geometry. Uniformity: consistent edge thickness and shape suggest uniform weld geometry, which is important for structural integrity. Irregularities: variations in edge thickness or shape may point to issues like excess weld material, undercutting, or burn-through.

Surface defect, porosity: small, irregular edges could indicate surface porosity or tiny holes in the weld. Spatter: additionally, unintended edges away from the main weld seam might be due to welding spatter.

Alignment and Fit-Up. Proper alignment: edges that follow a predictable, aligned path suggest that the welded components were properly aligned. Misalignment: deviations or offsets in the edge pattern can indicate misalignment or poor fit-up of the welded parts. Transition area: the edge detection can reveal the boundary between the weld region and the HAZ region, which is crucial for understanding the thermal impact on the material.

3. Thresholding is an effective process used to segment the image by converting it into a binary image. In this process, pixels are divided into two groups based on a chosen threshold value, and the pixels are then categorized into white and black. The method adopted is Global thresholding (Otsu's method), as it extracts more edges compared to direct edge detection algorithms

Global thresholding uses a common threshold value for the image under test. This value is applied uniformly to all pixels in the image. A threshold value is chosen, either manually or automatically. Adaptive thresholding involves estimation of the threshold value for segments of the image, thus resulting in variations of lighting and intensity where the image is divided into smaller regions or blocks. Global thresholding is best suited for simple images with uniform lighting, while adaptive thresholding is more versatile and effective for images with complex lighting conditions.

4. Image filtering: several methods are available for image filtering in the process of extracting the required image properties. The following methods are most commonly used in usual practice [24–33].

Gaussian blur: a linear filter that smoothens an image by averaging the pixels within a Gaussian window. It reduces noise and detail by weighting the pixels in the neighborhood based on a Gaussian function, which gives higher weights to the central pixels. It is suitable for blurring edges, reducing image sharpness. Not effective for non-Gaussian noise like salt-and-pepper noise. Best for overall noise reduction and obtaining a smooth image, but at the cost of blurring details. The Gaussian function is defined as: $G(x, y) = \frac{1}{2\pi\,\sigma^2} * e\left(-\frac{x^2+y^2}{2\sigma^2}\right)$, where σ is standard deviation of the Gaussian distribution.

Median filter: causes replacement of each pixel value with its neighborhood median value. Salt-and-pepper noise is effectively reduced by this filtering method, with no impact on the identified edges. For each pixel, the filter considers the values of all pixels in a neighborhood around it, sorts these values, and selects the median value. This filter removes salt-and-pepper noise and preserves edges better than linear filters like Gaussian blur. It is ideal for removing specific types of noise (e.g., salt-and-pepper) while preserving edges, useful for inspecting fine details and small defects in welded images.

Bilateral filter: the bilateral filter is an edge-preserving and noise-reducing filter that combines Gaussian smoothing in the spatial domain with Gaussian smoothing in the intensity domain. This ensures that only similar pixel values are averaged, preserving edges. The bilateral filter considers both the spatial distance and the intensity difference between the central pixel and its neighbors. Balances noise reduction with edge preservation, making it suitable for images where retaining the edge details is crucial. The filter function is: $I(x, y) = \frac{1}{W(x,y)} \sum_{x_i, y_i} I(x_i, y_i) \cdot e^{-\frac{(x_i-x)^2+(y_i-y)^2}{2\sigma_d^2}} \cdot e^{-\frac{(I(x_i,y_i)-I(x,y))^2}{2\sigma_d^2}}$, where σ_d is the spatial standard deviation, σ_r is the intensity standard deviation, and *W*(*x*,*y*) is a normalization factor.

Compared to the Gaussian and median filtering methods, the bilateral filter gives better results by preserving edges while reducing noise, which represents the quality of the edges formed duringthe welding process and is effective for a wide range of noise types. This makes the weld image analysis more accurate.

5. Texture analysis: texture analysis involves examining the texture characteristics of an image to extract meaningful information, which can be used for classification, segmentation, and other image processing tasks. Two commonly used methods are used in this work.

GLCM (gray-level co-occurrence matrix): this method is used to analyze an image texture by examining the spatial relationships between pixel intensities. GLCM analyzes texture by quantifying how frequently specific intensity value combinations appear in predetermined directional arrangements throughout the digital image matrix. Using this technique, several statistical measures can be calculated to describe the texture.

Contrast: quantifies tonal variation by calculating brightness differentials between adjacent data points throughout the entire visual matrix, enabling measurement of textural roughness across the image: $contrast = \Sigma_{i,j}(i-j)^2 \cdot P(i,j)$.

Correlation: measures the correlation of adjacent pixels, $correlation = \\ = \Sigma_{i,j} \frac{[(i-\mu_i)(j-\mu_j) \cdot P(i,j)]}{\sigma_i * \sigma j}$.

Energy (angular second moment): assesses uniformity of the texture by adding up the squared elements in the GLCM, $energy = \Sigma_{i,j} P(i,j)^2$.

Homogeneity (inverse difference moment): reflects the uniformity of pixel value relationships and distribution of elements in the GLCM cluster around the diagonal, $homogenity = \Sigma_{i,j} \frac{P(i,j)}{1+|i-j|}$.

Local binary patterns (LBP) is a texture operator that identifies patterns by evaluating adjacent pixel values against predetermined limits, enabling classification based on local spatial relationships within defined proximity boundaries. The LBP image is often represented as a histogram of the LBP codes, which serves as a texture descriptor.

6. Image segmentation: partitions the complete image into regions, making it easier to analyze and extract meaningful information. This process modifies the representation of an image into a form that is straight forward for analysis. Often by identifying objects or boundaries (lines, curves, etc.) within the image. The following methods are discussed in image segmentation.

K-means clustering: an unsupervised learning algorithm that is implemented to categorize data points into *K* clusters. In the context of image segmentation, it groups pixels based on their intensity or color similarity. The *K*-means clustering segments an image by grouping pixels into *K* clusters based on similarity in intensity or color. Simple and effective for basic segmentation tasks.

Watershed algorithm: a technique of segmentation in which the grayscale image is considered like a topographic surface. The algorithm finds the lines that separate different catchment basins, corresponding to the image regions. The Watershed Algorithm uses the topographic interpretation of the image to separate regions. Effective for segmenting touching or overlapping objects.

Graph-based segmentation: this technique treats the image as a graph, considering each pixel as a node, and the similarity between neighboring pixels is indicated by the edges. Segmentation is performed by finding minimum cuts in the graph based on pixel similarity. Offers flexible and powerful segmentation capabilities but may require more computational resources.

7. The entropy indicates the randomness to assess the degree of uncertainty in the image. Within the domain of image processing, entropy describes the texture and complexity of an image. An image with high entropy is characterized by intricate Higher entropy values indicate a more complex and detailed image, while lower entropy values suggest a more uniform or simple image. The entropy *H* of an image can be calculated using the following equation: $H = -\Sigma_{i=1\ to\ n} p_i \log_2(p_i)$, where *n* is the count of variations in intensity in the image and 'pi' is the probability at which intensity of level I occurs.

Entropy is used to analyze and classify textures in an image. Entropy-based methods can be used to determine optimal thresholds for image segmentation. High entropy characterized by intricate details and complexity, while low entropy indicates a uniform or simple image. Entropy can be used as a feature for image recognition and classification tasks.

8. Fourier transform: in image processing, the Fourier Transform is a fundamental tool used to analyze the frequency components present in an image. Here's a concise explanation of what the Fourier transform entails. The Fourier transform converts a signal (in this case, an image) from its spatial domain into the frequency domain. It decomposes the image into its constituent frequencies. For a 2D image *f(x,y)*, the Fourier transform *F(u,v)* is given by: $F(u,v) = \iint_{-\infty}^{\infty} f(x,y)\, e^{-i2\pi(ux+vy)}\, dx \cdot dy$, where *u* and *v* are wavenumber components.

The magnitude variation of an image refers to the representation of the magnitude (absolute value) of the Fourier transform coefficients of the image. The phase spectrum of an image refers to the spatial distribution of phase information in the frequency domain of the image.

Results and Discussion

The analysis was carried out on four SEM images, and the interpretations for the various techniques of preprocessing are described in this section.

Histogram of weld images

Peaks indicate common intensity values. A narrow histogram suggests low contrast, while a wide histogram suggests high contrast. Expanding the range of intensity values makes images clearer, more detailed, and more suitable for visual inspection and automated analysis. The image in its stretched form and the corresponding histogram (Figs. 4 and 5) for samples 2H and 1C, indicate clear contrasting features of the image where the lack of fusion, slag formation, cracks, and unfilled gaps can be identified. These characteristics indicate the defects in the weld piece, which creates a non-uniform surface on the weld piece. While the histogram in Fig. 6 (for sample 3H) indicates no defect in the weld, corresponding to the sample performance, as listed in Table 1 [17].

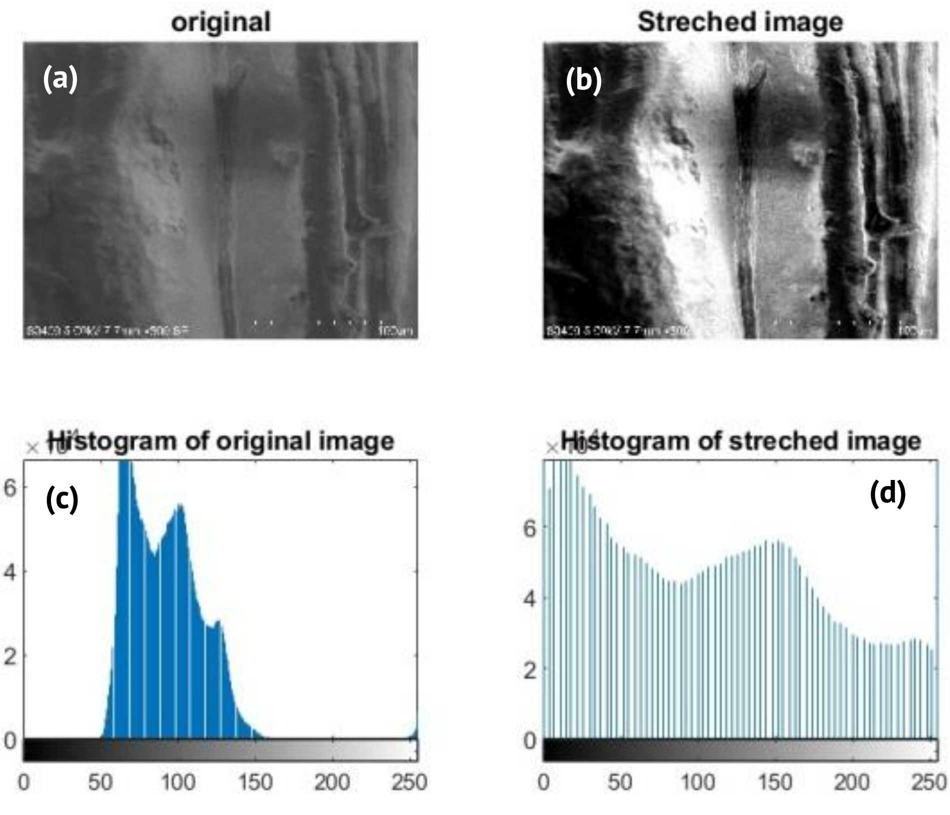

Fig. 4. SEM image of sample 2H (a,b) and its histogram stretched image (d) and its histogram (c)

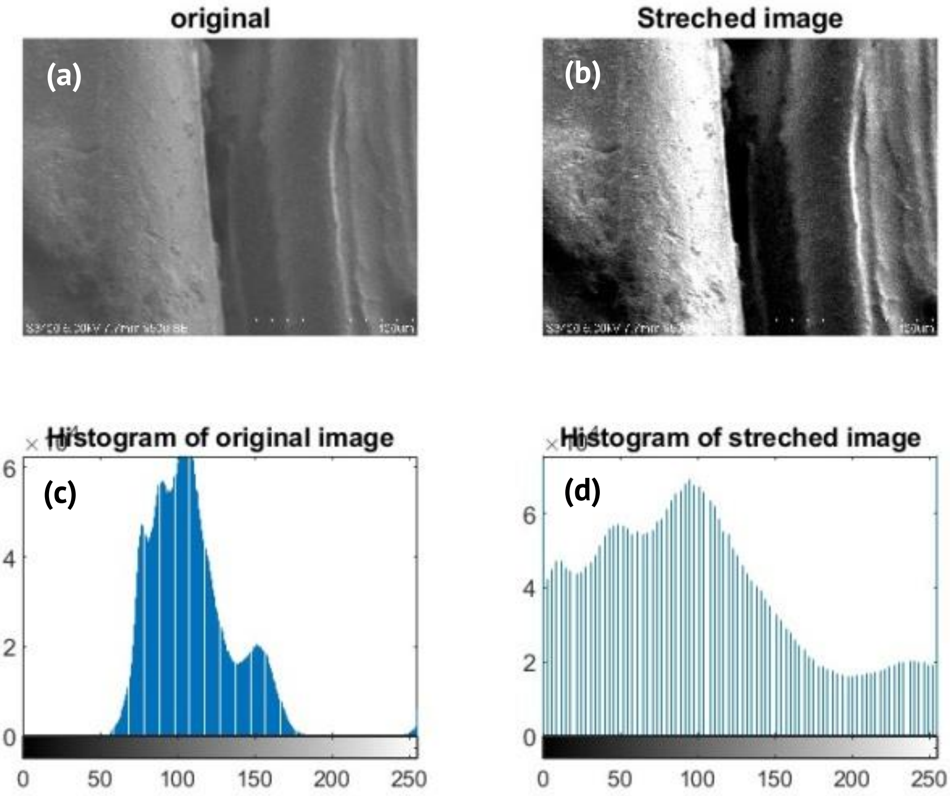

Fig. 5. SEM images of sample 1C (a,b) and its histogram stretched image (d) and its histogram (c)

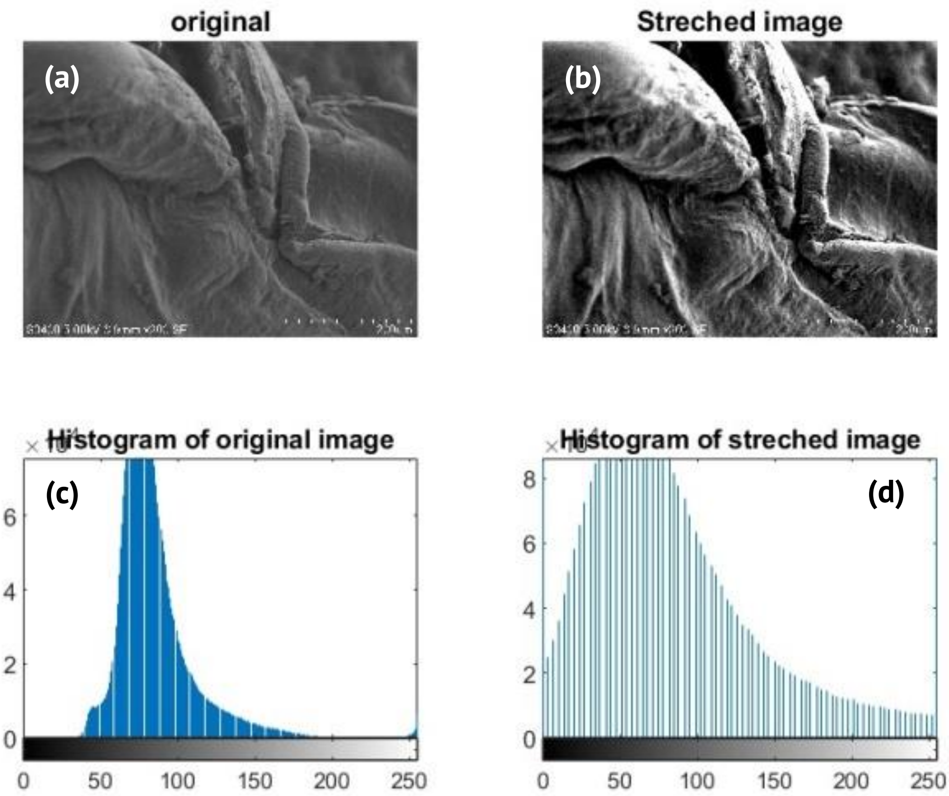

Fig. 6. SEM images of sample 3H (a,b) and its histogram stretched image (d) and its histogram (c)

Interpretation from edge detection

Figures 7 and 8 show the edge detection of samples 2F and 3H using their SEM images by the Roberts Cross Operator algorithm**,** which uses 2 × 2 convolution kernels to approximate the gradient. The edges seen in the images represent discontinuities in the weld formation that may be attributed to anomalies like slag, unfused, and uncut surfaces in the image, the whiter dots, the more the edge formation during welding. The clear image without white heads may indicate fewer discontinuities in the weld formation. These results indicate a contradiction to the actual weld performance and may indicate the need for further detailed analysis of the image processing results and inferences.

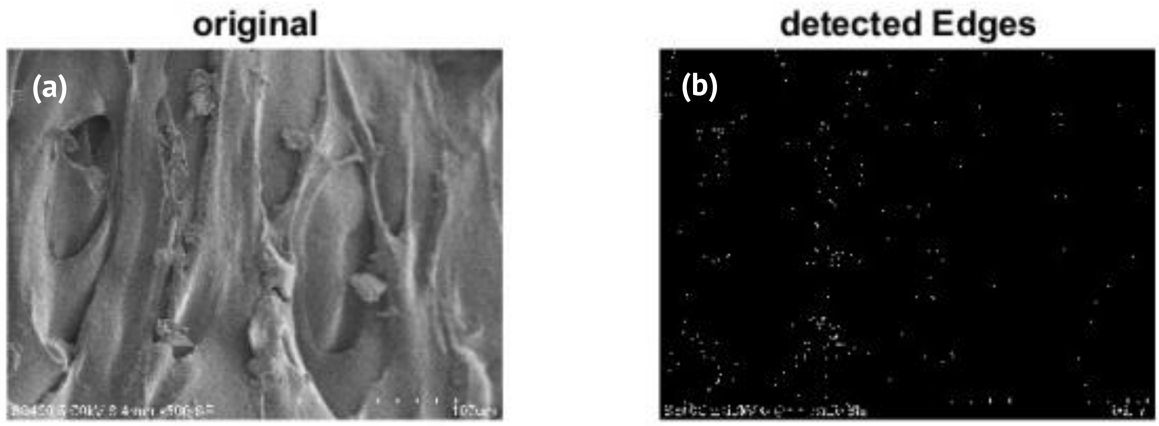

Fig. 7. SEM image surface of sample 3H (a) and edge detection image (b) for sample 3H

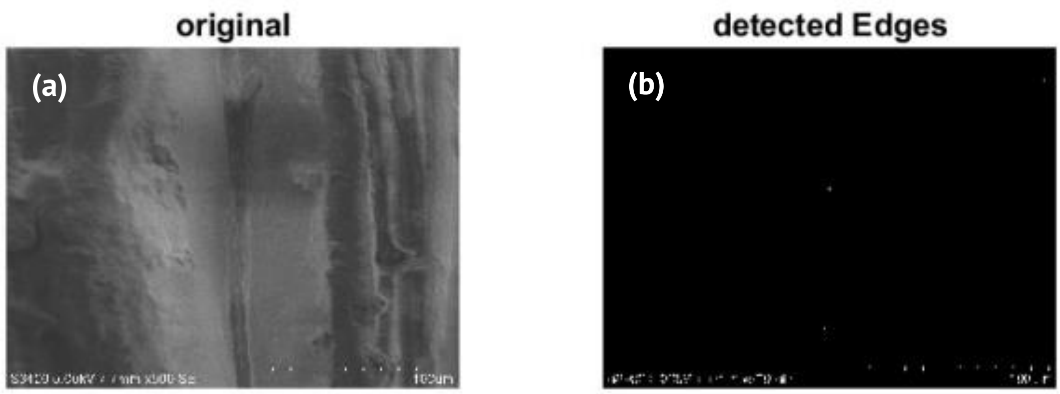

Fig. 8. SEM image surface of sample 2F (a) and edge detection image (b) for sample 2F

Interpretation from thresholding

Thresholding helps to isolate the weld bead from the rest of the image. This is vital for the assessment of the weld characteristics of quality, size, and shape.

Detection of anomalies like porosity, cracks, or incomplete fusion can be done with thresholding. Defects usually have different intensity values than the rest of the weld, making them stand out after thresholding.

Contrast enhancement makes it easier to inspect and analyze the weld visually. This is particularly useful in cases where the weld and the surrounding material have similar intensity values in the original image.

The thresholding image for Sample 3I, in Fig. 9, indicates the slag formed after welding, and the bulged surfaces can be seen more clearly, which represents the over-welding with improper finishing surfaces showing the white edges of excessive material spread. The welding status of sample 3I shows the weld to have caused overheating of the material, which is due to the higher parametric range than other samples.

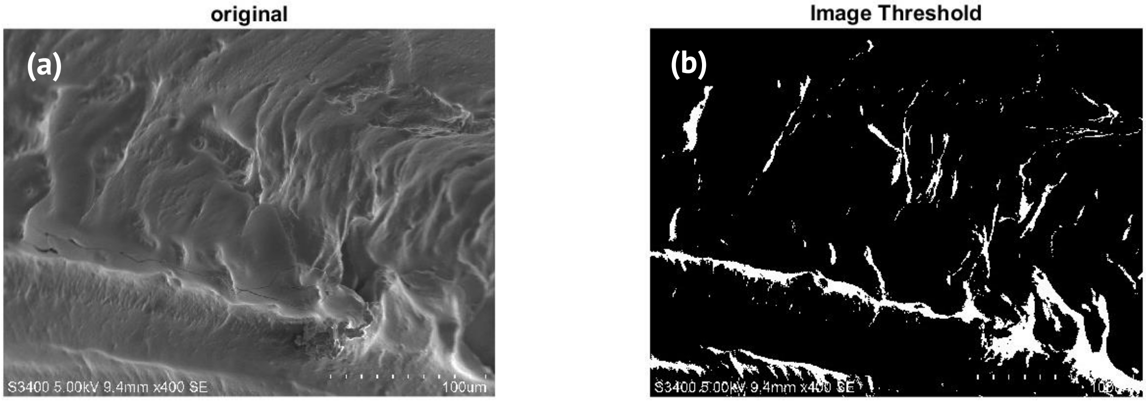

Fig. 9. Original SEM image (a) and its processed threshold (b)

Filtering output

The filtering output for the SEM image of sample 2B, Fig. 10, has been analyzed in this section for the changes in texture properties with spatial factors. The common image filtering techniques were utilized, namely Gaussian blur, median filtering, and bilateral filtering, for noise removal and smoothing of the images. The smoothing effect differs in the form of uniform, non-linear, or adaptive smoothing [24]. The following features are obtained from the above image.

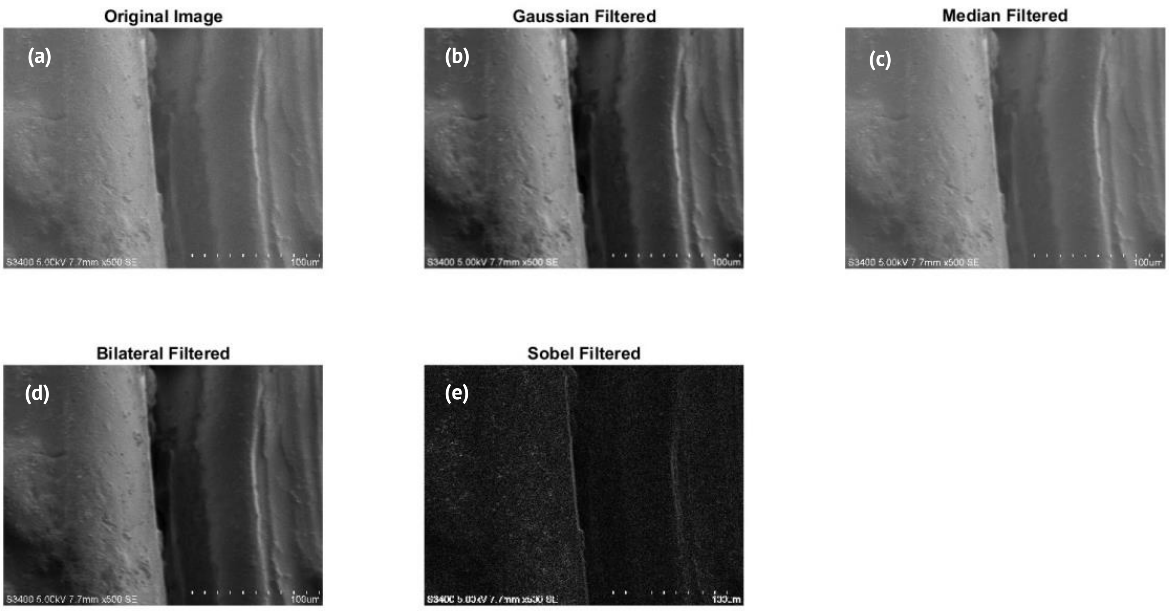

Fig. 10. SEM Images of Sample 2B filtered with different standard filtering methods (a–e)

GLCM features: GLCM is computed at specific spatial relationships defined by:
1. Directions: horizontal (0°), vertical (90°), diagonal (45°), anti-diagonal (135°), etc.
2. Distances: the number of pixels apart being analyzed. The matrix values thus represent how the texture property (e.g., contrast, correlation, etc.) changes with the analyzed direction/distance.
3. Contrast: [0.1255 0.1865 0.1336 0.1778].
4. Correlation: [0.8992 0.8502 0.8927 0.8571].
5. Energy: [0.4564 0.4319 0.4439 0.4358].
6. Homogeneity: [0.9613 0.9397 0.9510 0.9444]

Contrast in an image represents the difference in luminance or color that makes an object distinguishable. The correlation value shows the linear dependency of pixel intensities for a specific direction/distance. The high values indicate that pixel intensities are strongly related, regardless of direction or distance. Energy value reflects the uniformity of texture for a specific direction/distance. The moderate values suggest a somewhat uniform texture, but not perfectly repetitive. Homogeneity value measures how close pixel intensities are to one another for a given direction/distance. The high values indicate high similarity of neighboring pixel intensities in all directions, showing a smooth texture. Together, these values describe the variation of texture properties across different spatial relationships in the analyzed image.

Interpretation from the texture analysis

LBP (local binary patterns): the histogram shows the frequency of each LBP code in the SEM image of sample 3H (Fig. 11).

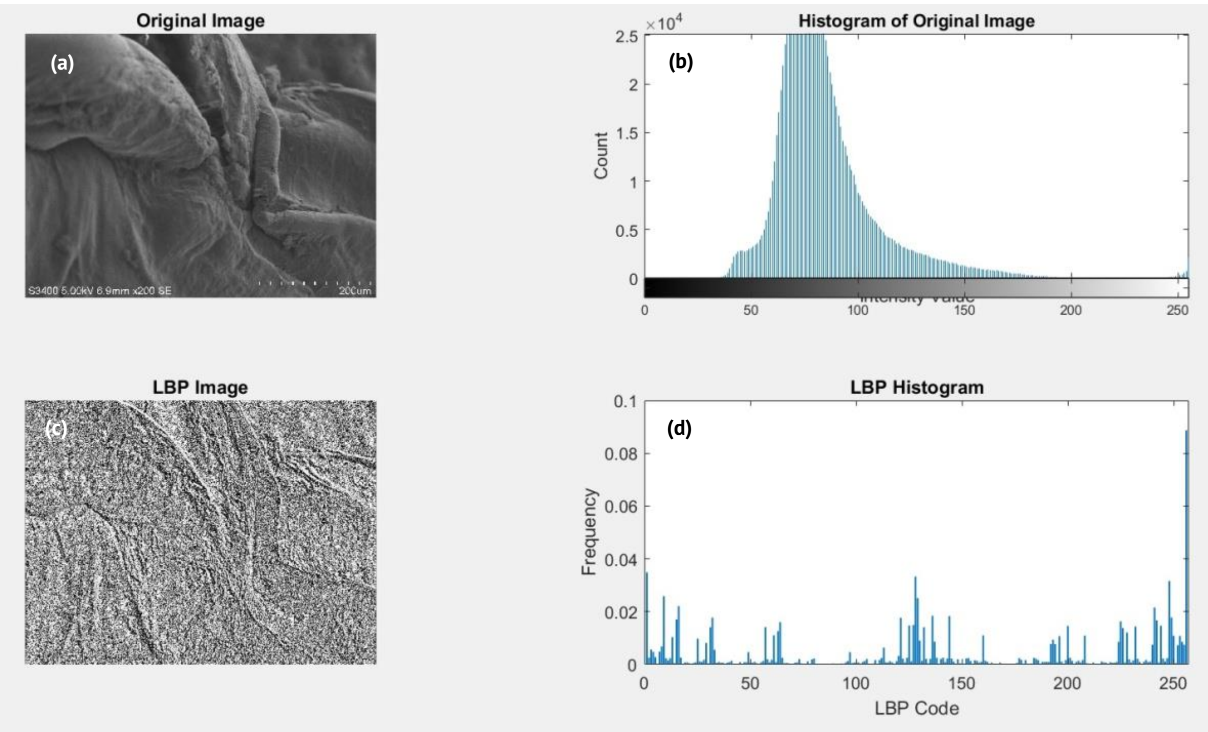

Fig. 11. Histogram of original (a,b) and LBP image (c,d)

From the above histograms of the original image and the LBP histogram, it's clear that the LBP histogram is more stretched than the original histogram, representing more edges on the image, implying non-uniform weld quality. By combining GLCM features from image filtering and LBP features from the texture analysis, a comprehensive understanding of the welded image texture can be obtained.

1. Consistency and quality: high homogeneity, high energy, high correlation (from GLCM), and a peaked LBP histogram with many uniform patterns suggest a high-quality weld with a smooth, consistent texture.

2. Defects and irregularities: high contrast, low homogeneity, low correlation (from GLCM), and a flat LBP histogram with many non-uniform patterns can indicate defects, roughness, or irregularities in the weld texture.

3. Surface properties: detailed examination of specific GLCM features like contrast and homogeneity, along with the LBP histogram, can help identify specific types of surface properties, such as the presence of cracks, porosity, or other surface defects.

Interpretations from image segmentation

The image segmentation technique was utilized for separating the features or regions of the SEM image of sample 2B. Figure 12 shows the result of image segmentation obtained with the above-mentioned techniques for sample 2B.

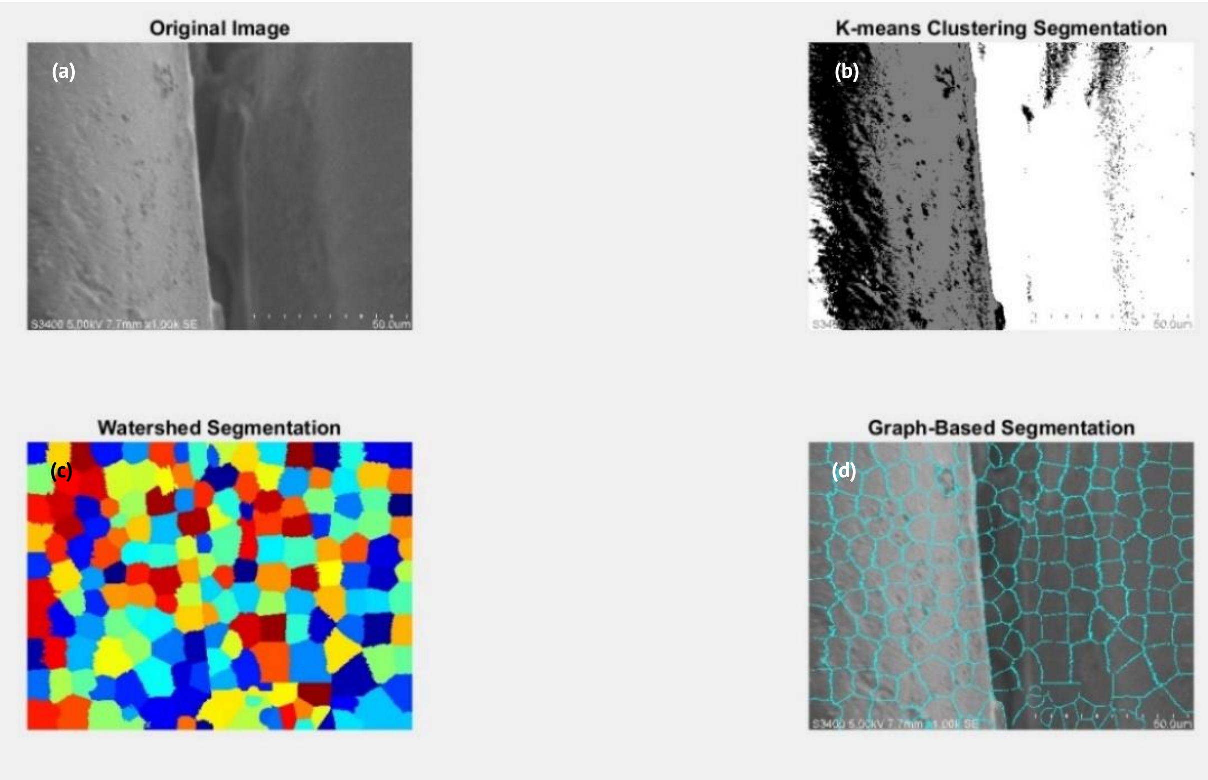

Fig. 12. Original SEM image of sample 2B (a) and results of K-means, watershed, and graph-based image segmentation (b–d)

The splitting of the SEM image into sections and the color gradations give an idea about the discontinuities in the weld formation, and also the difference in grain distribution as a result of the thermal gradients created due to the friction and viscous heat created between the weld surfaces in the process of ultrasonic welding.

Entropy interpretation

An image with high entropy will show a complex scene with many details and textures, and its entropy value will be relatively high. Low-entropy image will show a uniform or simple scene. By comparing these entropy values, the complexity and information content of the images can be interpreted. Figure 13 represents the entropy values for samples 2B and 3H.

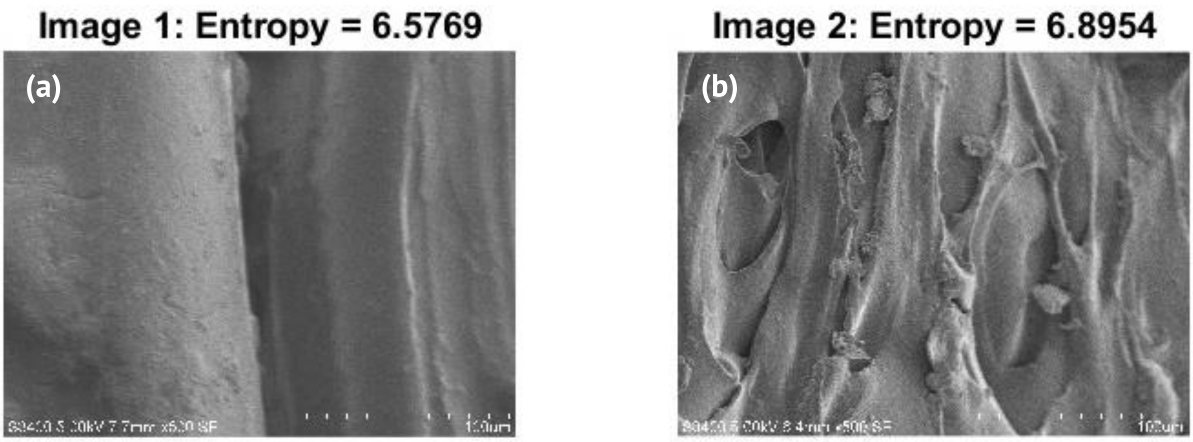

Fig. 13. Entropy values for the samples 2B (a) and 3H (b)

In Fig. 13(b), Image 2 has higher entropy (6.8954) compared to Image 1 (6.5769). This indicates that Image 2 has more complexity or randomness, which may be interpreted as a strong molecular bonding of the two weld pieces, as is observed in the weld performance of sample 3H.

Interpretation from the Fourier transform

Fourier transformation conveys information about the spatial frequency content of the image: Low frequencies represent areas of uniform intensity, representing smooth regions in the source image. High frequencies correspond to rapid changes in intensity, indicating edges or textures.

Fourier transform conducted on the SEM images of sample 3H, Fig. 14 indicates the components for all frequencies, with magnitude reducing for higher frequencies. The logarithmically transformed image also suggests the dominating directions, one vertical and one horizontal, in the Fourier image, both passing through the center. This infers a regular pattern of grain distribution in the baseline SEM image of sample 3H, confirming the status as obtained with the parameter settings of sample 3H.

The results obtained with the various image processing techniques applied to a small set of SEM images are observed to be either in sync or in variation with the destructive testing performance of the weld samples. This observation requires further analysis of these techniques applied to a larger set of SEM images to arrive at a definite

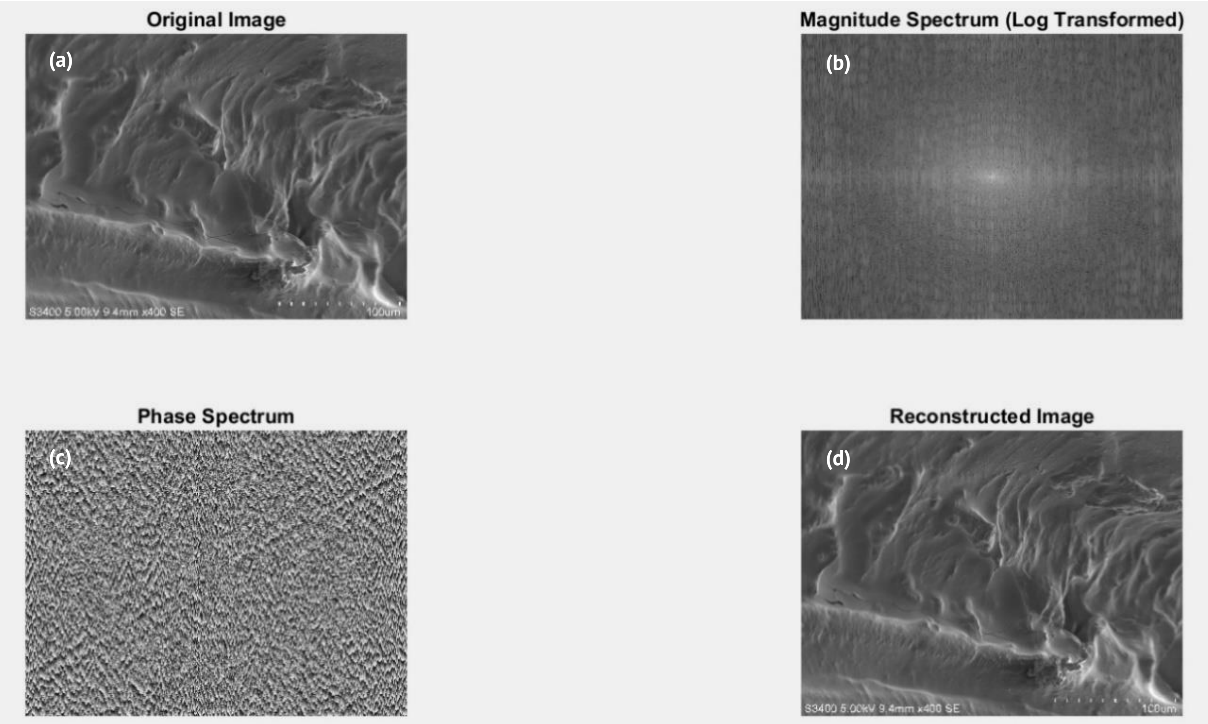

Fig. 14. Original SEM image of sample 3H (a) and Fourier transform output images (b–d)

pattern for the optimal selection of image processing techniques for weld defect detection. The variation in the results may be attributed to the broad range of non-uniformities in the weld formation due to thermal gradients, which usually result in varied characteristics. This makes it challenging to develop a generalized method of image-based defect detection. The characteristics of defects, like their appearance as regions of low contrast, non-uniform brightness, or irregular shapes, may result in anomalies in their detection.

Conclusions

Applying image processing techniques in the characterization and defect detection of weld samples using SEM images has significant potential toimplement automation in the weld defect detection domain. With further refinement of the analysis and detailed study, the image processing techniques can be effectively used for defect detection with the sample SEM images for welds formed with varying parametric levels. Techniques such as image segmentation, thresholding, and edge detection play a crucial role in isolating relevant features within complex microstructures, allowing for a more precise analysis of weld integrity. Furthermore, entropy detection aids in identifying anomalies by quantifying information variability, which is essential for assessing the quality of welds. The Fourier transform contributes to identifying periodic structures and defects, enhancing our understanding of the weld's mechanical properties. Additionally, texture analysis provides insights into the surface characteristics and microstructural variations, crucial for predicting performance under various conditions. Filtering techniques help in noise reduction, ensuring that the subsequent analysis reflects true structural characteristics rather than artifacts.

Collectively, these image-processing techniques enable a comprehensive assessment of weld quality, facilitating early detection of defects that could compromise structural integrity. This research underscores the importance of integrating advanced image processing methods into quality control processes in manufacturing, thereby enhancing reliability and safety in critical applications. The findings illustrate the potential for further advancements in the field, opening avenues for automation in defect detection methodologies. The following interpretations and guidelines can be deduced from the image processing algorithms discussed above:

1. The impact and significance of an algorithm can be assessed with a comparison of the original and processed Images.
2. Parameter sensitivity analysis can be effectively made with the variation of the algorithmic parameters and analysis of the change in results, e.g., threshold values in segmentation.
3. Algorithm performance can be quantitatively evaluated using metrics like precision, recall, or mean squared error, especially in machine learning and computer vision tasks.

Analysis and interpretation of errors introduced by the algorithm can guide improvements or alternative approaches. By systematically evaluating these aspects, we can effectively interpret image processing results from different algorithms, ensuring that they meet the desired goals and quality standards.

Credit authorship contribution statement

G.C. Ganesha iD Sc R: experimentation, simulation and writing; **Chaturvedi Mukti** iD Sc R: conceptualization, design of experiments, experimentation, paper writing, validations; **Arungalai Vendan Subbiah** iD Sc R: conceptualization, design of experiments, experimentation, paper writing, validations; **Radder Sharanabasavaraj** iD Sc R: testing and characterization, simulation, experimentation.

Conflict of interest

The authors declare that they have no conflict of interest.

References

1. Xu Y, Fang G, Chen S, Zou JJ, Ye Z. Real-time image processing for vision-based weld seam tracking in robotic GMAW. *Int J Adv Manuf Technol.* 2014;73: 1413–1425.
2. Nacereddine N, Zelmat M, Belaifa SS, Tridi M. Weld defect detection in industrial radiography based digital image processing. *Transactions on Engineering Computing and Technology*. 2005;2: 145–148.
3. Liao G, Xi J. Image processing technology for pipe weld visual inspection. In: *2009 WASE International Conference on Information Engineering*. IEEE; 2009. p.173–176.
4. Yang SM, Cho MH, Lee HY, Cho TD. Weld line detection and process control for welding automation. *Measurement Science and Technology*. 2007;18(3): 819.
5. Roca Barceló F, Jaén del Hierro P, Ribes Llario F, Real Herráiz J. Development of an ultrasonic weld inspection system based on image processing and neural networks. *Nondestructive Testing and Evaluation*. 2018;33(2): 229–236.
6. Li Y, Hu M, Wang T. Weld image recognition algorithm based on deep learning. *International Journal of Pattern Recognition and Artificial Intelligence*. 2020;34(08): 2052004.
7. Pan H, Pang Z, Wang Y, Wang Y, Chen L. A new image recognition and classification method combining transfer learning algorithm and mobilenet model for welding defects. *IEEE Access*. 2020;8: 119951–119960.

8. Sun J, Li C, Wu XJ, Palade V, Fang W. An effective method of weld defect detection and classification based on machine vision. *IEEE Transactions on Industrial Informatics.* 2019;15(12): 6322–6333.
9. Wang G, Liao TW. Automatic identification of different types of welding defects in radiographic images. *Ndt& E International.* 2002;35(8): 519–528.
10. Ranjan R, Khan AR, Parikh C, Jain R, Mahto RP, Pal S, Pal SK, Chakravarty D. Classification and identification of surface defects in friction stir welding: An image processing approach. *Journal of Manufacturing Processes.* 2016;22: 237–253.
11. Kumar RK, Omkumar M. Investigation and characterization of ultrasonically welded GF/PA6T composites. *Materials Today: Proceedings.* 2020;26: 282–286.
12. Mohammad EJ. Image processing of SEM image nano silver using K-means MATLAB technique. *Al-Mustansiriyah Journal of Science.* 2019;29(3): 150–157.
13. Shaikh K, Hussain I, Chowdhry BS. Wheel defect detection using a hybrid deep learning approach. *Sensors.* 2023;23(14): 6248.
14. Tata RK, Brahma Rao KBV. Hybrid CNN-LSTM Architecture for Automated Defect Detection in Industrial Surface Inspection. *Multidisciplinary Journal for Applied Research in Engineering and Technology.* 2025;5(1): 11–16.
15. Wang X, Gao S, Guo J, Wang C, Xiong L, Zou Y. Deep learning-based integrated circuit surface defect detection: Addressing information density imbalance for industrial application. *International Journal of Computational Intelligence Systems*. 2024;17(1): 29.
16. Mu W, Gao J, Jiang H, Wang Z, Chen F, Dang C. Automatic classification approach to weld defects based on PCA and SVM. *Insight-Non-Destructive Testing and Condition Monitoring.* 2013;55(10): 535–539.
17. Khalifa W, Abouelatta O, Gadelmawla E, Elewa I. Classification of Welding Defects Using Gray Level Histogram Techniques via Neural Network. *MEJ-Mansoura Engineering Journal.* 2020;39(4): 11.
18. Rathod VR, Anand RS. A comparative study of different segmentation techniques for detection of flaws in NDE weld images. *Journal of Nondestructive Evaluation.* 2012;31: 1–16.
19. Rajab MI, El-Benawy TA, Al-Hazmi MW. Application of frequency domain processing to X-ray radiographic images of welding defects. *Journal of X-Ray Science and Technology.* 2007;15(3): 147–156.
20. Srinivasan K, Kumaran SS. Quality assessment of friction welding using image super-resolution via deep convolutional neural networks. *Materials Today: Proceedings.* 2020;22: 2266–2273.
21. Chu HH, Wang ZY. A vision-based system for post-welding quality measurement and defect detection. *The International Journal of Advanced Manufacturing Technology.* 2016;86: 3007–3014.
22. Xu H, Yan ZH, Ji BW, Huang PF, Cheng JP, Wu XD. Defect detection in welding radiographic images based on semantic segmentation methods. *Measurement.* 2022;188: 110569.
23. Hou W, Zhang D, Wei Y, Guo J, Zhang X. Review on computer aided weld defect detection from radiography images. *Applied Sciences.* 2020;10(5): 1878.
24. Cheng Y, Deng H, Feng Y, Xiang J. Weld defect detection and image defect recognition using deep learning technology. Researchsquare [Preprint]. Available from: doi.org/10.21203/rs.3.rs-149365/v1.
25. Civcik L, Aksin MA. Image Enhancement in Industrial Welding Environment With Image Processing Techniques. *Konya Journal of Engineering Sciences.* 2025;13(1): 238–259.
26. Chen Y, Li L, Chen F, Chen J. Application and prospect of image processing in welding. *Material Science and Technology.* 2003;11(1): 106–112.
27. Foorginejad A, Mohammad Emam S, Jamshidi H, Ranjbar S. Image processing technique for measuring the weld dilution and heat-affected zone to model the gas metal arc welding process by a neuro-fuzzy system. *Journal of Optical Technology.* 2023;90(12): 743–752.
28. Deng L, Guo Y, Chai B. Defect detection on a wind turbine blade based on digital image processing. *Processes.* 2021;9(8): 1452.
29. Ren Z, Fang F, Yan N, Wu Y. State of the art in defect detection based on machine vision. *International Journal of Precision Engineering and Manufacturing-Green Technology.* 2022;9(2): 661–691.
30. Argunova TS, Kohn VG, Roshchin BS, Nuzhdin AD, Lim JH, Lebedev SP, Ankudinov AV. Surface study by x-ray scattering technique and phase contrast imaging: the examples of graphene and sapphire. *Materials Physics and Mechanics.* 2024;52(5): 64–73.
31. Pozdnyakov AO, Sedakova EB. Thermal analysis of wear of polymer-polymer friction pairs in vacuum and atmosphere conditions. *Materials Physics and Mechanics.* 2024;52(4): 63–80.
32. Erofeev DA, Pirozhnikov PB, Keresten IA, Titov AG. Experimental determination of physical, chemical and surface properties of biocompatible thermoplastic. *Materials Physics and Mechanics.* 2024;52(3): 1–12.
33. Singh DP, Dwivedi VK, Agarwal M. Optimizing processing parameters for semi-solid casting: a comprehensive review. *Materials Physics and Mechanics.* 2024;52(2): 1–10.